

## Performance of AMANDA-II using Transient Waveform Recorders

A. Silvestri for the IceCube Collaboration

*Department of Physics and Astronomy, University of California, Irvine, CA 92697, USA*

Presenter: Timo Messarius (silvestri@HEP.ps.uci.edu), usa-silvestri-A-abs1-og27-poster

AMANDA-II data acquisition electronics was upgraded in January 2003 to readout the complete waveform from the buried PMTs using Transient Waveform Recorders (TWR). We perform the same atmospheric neutrino analysis on data collected in 2003 by the TWR and standard AMANDA data acquisition system ( $\mu$ -DAQ). Good agreement in event rate and angular distribution verify the baseline performance of the TWR system.

### 1. Description of $\mu$ -DAQ and TWR-DAQ Systems in AMANDA

The Antarctic Muon And Neutrino Detector Array (AMANDA) is the first neutrino telescope constructed in transparent ice, and deployed between 1500 m and 2000 m beneath the surface of the ice at the geographic South Pole in Antarctica. AMANDA-II [1] was completed in February 2000 and has taken data routinely since that time [2]. It is designed to search for neutrinos that originate in the most violent phenomena in the observable universe. AMANDA has searched for point sources in the entire northern sky and for diffuse sources of high energy neutrinos of cosmic origin.

Since 1997 the detector is taking data using a data acquisition electronics based on Time to Digital Converters (TDC) which measures the arrival time of the PMT pulses, and Analog to Digital Converters (ADC), which record the maximum value of the PMT pulse amplitude. Limitation of this system are the TDC with a maximum of 8 leading edges per trigger, and the peak ADC that records only one amplitude per event. The limitation is particularly acute for bright, high energy events, because important information on afterpulses is lost. The data acquisition electronics of the AMANDA-II detector was upgraded in 2003 to readout the complete waveform of the photomultiplier tubes (PMTs) using Transient Waveform Recorders (TWR) [3]. Afterpulse information is crucial to extend the dynamic range of Number of photo-electron ( $N_{pe}$ ) measurement up to 5000 photons [3].

In order to distinguish the two data acquisition electronics of the AMANDA detector, we call  $\mu$ -DAQ the original system operating since 2000, and TWR-DAQ the upgraded system using waveforms since 2003. The decision was made to run the two systems in parallel until the TWR-DAQ was proven to work as satisfactorily. To compare the two systems the data from 2003 has been analyzed with both read-out systems. Additional information on the TWR-DAQ hardware can be found in [4].

Extending the analysis tools to include TWR data required several new developments: (1) The TWR-DAQ measures the integrated charge  $Q$  of the PMT pulses. In contrast, the  $\mu$ -DAQ only measures the maximum amplitude of the PMT waveform in a  $2 \mu s$  window. (2) We account for various time offsets and we extract a timing resolution of few nanoseconds. The performance of the TWR-DAQ is tested by comparing the results for the absolute rate of atmospheric neutrinos and the  $\cos(\theta)$  distribution with the results from the standard  $\mu$ -DAQ.

### 2. Data Processing and Comparison of $\mu$ -DAQ and TWR-DAQ Systems

The TWR-DAQ data volume reaches 15TB per year compared to  $\sim 1$ TB of the  $\mu$ -DAQ system. The data information of the two systems has been merged according to GPS time and the fraction of overlapping PMTs participating in the event in both systems. For this analysis we restricted the capabilities of the TWR-DAQ

system to mimic the features of the  $\mu$ -DAQ system as close as possible. The timing and amplitude information extracted from waveforms has been used as input parameters to perform PMT-pulse cleaning, TOT (Time-Over-Threshold) and cross-talk cleaning.

Due to small differences in threshold values, the TWR-DAQ collects  $\sim 80\%$  of pulses observed in the  $\mu$ -DAQ system.<sup>1</sup> A software re-trigger was applied at lower majority ( $M = 19$ ) to obtain similar rates after PMT-pulse cleaning procedures. TOT-cleaning procedures were tested using  $\mu$ -DAQ data, which exclude anomalous PMT-pulses which are too short or too long. The same TOT-cleaning was performed on the TWR-DAQ data, which causes a slight loss in efficiency due to the higher threshold. Cross-talk cleaning procedures were also tested using  $\mu$ -DAQ data, and cross-talk tables were designed according the ADC and TOT response observed in  $\mu$ -DAQ data. We decided to apply the same cross-talk cleaning procedures to perform a closer comparison, however small differences are expected since the  $\mu$ -DAQ data contains differences TOT values, and peak ADC are replaced by the integrated charge  $Q$ .

Timing and amplitude calibration have been performed using a threshold algorithm which captures the leading and trailing edge of single PMT pulses, and calculate the Npe from integrated charge. Time offsets are calculated and have been applied as  $t_{offset} = t_{cable} - t_{module} - t_{delay} - t_Q$ , where  $t_{cable}$ ,  $t_{module}$ ,  $t_{delay}$  and  $t_Q$  account for cabling offset, TWR module hardware clock, stop delay of trigger response and amplitude-timing corrections, respectively. Amplitude-timing corrections are performed by fitting the leading edge versus  $1/\sqrt{Q}$ , where  $Q$  is the integrated charge rather than peak ADC measurement. These measurements are then compared to the standard timing calibration of the  $\mu$ -DAQ.

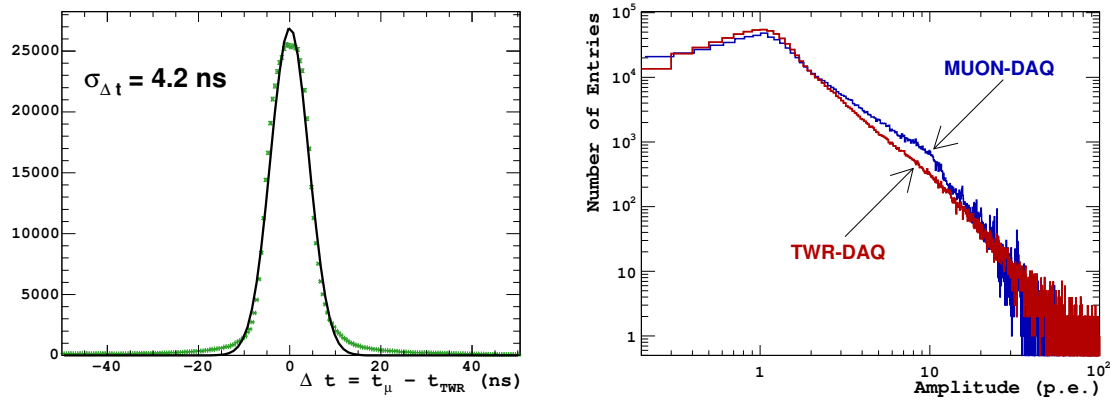


**Figure 1.** (Left) Time difference between the PMT pulses recored by the two acquisition systems  $\Delta t = t_\mu - t_{TWR}$ . (Right) Calibrated amplitude normalized to 1 photo-electron (p.e.) value for  $\mu$ -DAQ and TWR-DAQ data. See text for details

A Gaussian fit of the distribution for  $\Delta t = t_\mu - t_{TWR}$  yields  $\sigma_{\Delta t} = 4.2$  ns (Figure 1 (left)), which is dominated by the systematic error of the time jitter between independent flash ADC clocks of the TWR system. The TWR-DAQ timing calculations are relative to the values measured by the  $\mu$ -DAQ. The timing of the TWR-DAQ system includes two sources of jitter, both are related to a uniform window that is 10 ns in duration. This account for the  $\sigma_{\Delta t} \sim 4$  ns. Amplitudes are also calibrated by extracting the number of photo-electron (Npe) detected from peak ADC of the  $\mu$ -DAQ and charge  $Q$  of the TWR system and normalized to 1pe amplitude.

<sup>1</sup>The pulse detection efficiency was increased in 2004 and 2005 seasons.

By integrating the charge from pulse in the waveform, the dynamic range of the TWR-DAQ extends to  $N_{pe} \sim 100$ , to be compared to  $N_{pe} \sim 30$  of the  $\mu$ -DAQ. Figure 1 (right) shows the reconstructed amplitude of the TWR-DAQ compared to the  $\mu$ -DAQ, which indicates a stable power law distribution extending up to 100  $N_{pe}$ , while the  $\mu$ -DAQ system shows a “knee” around 10  $N_{pe}$ . The knee is due to the amplitude saturation of the channels with optical fibers, approximately 40% of the AMANDA readout.<sup>2</sup> After cleaning, the muon track is reconstructed from the remaining information. Details on the reconstruction techniques can be found in [5]. Table 1 summarizes the passing rates from the raw data level to the final sample of atmospheric neutrinos.

**Table 1.** Passing rates for increasing cut selection level for the TWR-DAQ and  $\mu$ -DAQ data analysis.

Selection	TWR-DAQ	$\mu$ -DAQ
Raw Sample	$1.86 \times 10^9$	$1.86 \times 10^9$
Level-1	$1.25 \times 10^8$	$1.25 \times 10^8$
Level-3	$2.56 \times 10^6$	$1.99 \times 10^6$
Final Sample	1112	1026

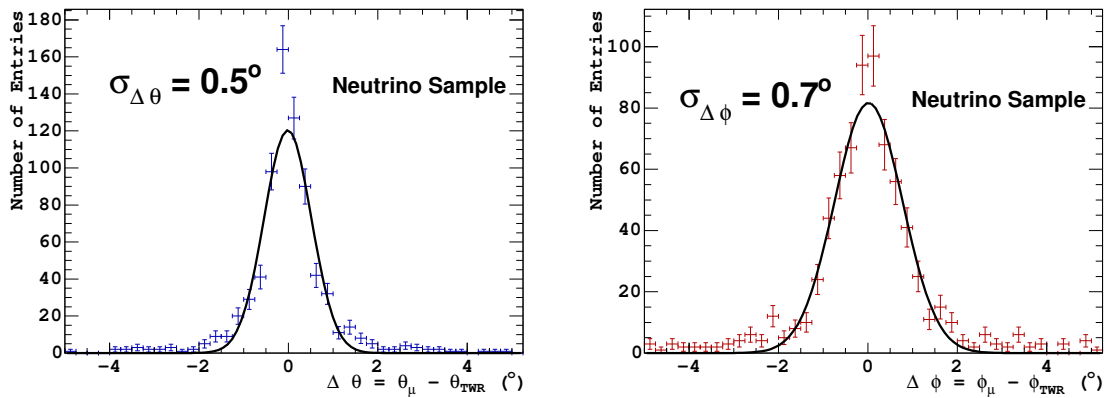


**Figure 2.** (Left) The zenith  $\Delta\theta = \theta_\mu - \theta_{TWR}$  difference distribution between the  $\mu$ -DAQ and the TWR-DAQ systems, (right) the azimuthal  $\Delta\phi = \phi_\mu - \phi_{TWR}$  difference distribution.

Figure 2 shows that the angular mismatch for the final neutrino sample,  $\sigma_{\Delta\theta}$  is  $0.5^\circ$ , where  $\Delta\theta = \theta_\mu - \theta_{TWR}$ . This value is expected from studies of the precision of the global minimizer in the reconstruction program. From the analysis based on TWR-DAQ data, 1112 neutrinos are observed compared to 1026 neutrinos from the  $\mu$ -DAQ data analysis. The small differences in the event rate are compatible with the small differences in analysis procedures described in Section 2.

Figure 3 shows the  $\cos\theta$  distribution of the atmospheric neutrino sample extracted from the TWR-DAQ and  $\mu$ -DAQ data analysis. Satisfactory agreement can be seen for the  $\cos\theta$  distribution of the atmospheric neutrinos samples obtained by the different analyses.

<sup>2</sup>High voltage values have been lowered in January 2005 to increase linear dynamic range of optical channels.

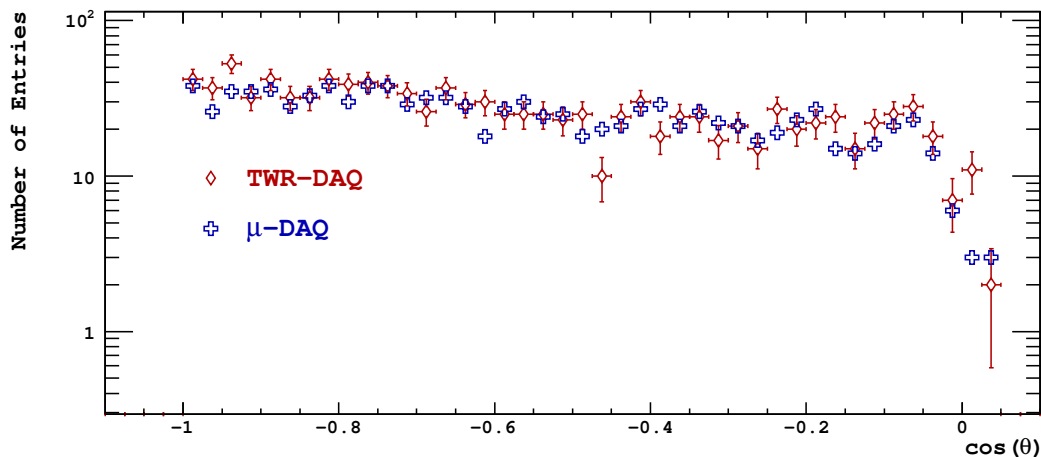


**Figure 3.**  $\cos\theta$  distribution after final cut level representing the atmospheric neutrino sample observed from the TWR-DAQ and the  $\mu$ -DAQ analyses.

### 3. Discussion and Conclusion

The atmospheric neutrino analysis provides the first detailed evaluation of the performance of the TWR-DAQ system. The preceding discussion demonstrated that the TWR-DAQ produces similar event rates and angular distribution as the data collected by the standard  $\mu$ -DAQ system. This encouraging result was obtained by first converting the waveforms into the more restricted information collected by the  $\mu$ -DAQ. At that point, the standard AMANDA analysis tools were applied to data from both of the electronic systems, although some of the procedures were reformulated to process waveform information.

We are developing new software tools to exploit the full information contained in the waveform. We expect that the additional information will improve energy and angular resolution crucial for the search of high energy phenomena.

### 4. Acknowledgements

The author acknowledges support from the U.S. National Science Foundation Physics Division, the NSF-supported TeraGrid systems at the San Diego Supercomputer Center (SDSC), and the National Center for Supercomputing Applications (NCSA).

### References

- [1] M. Ackermann et al., Phys. Rev. D, 71:077102 (2005).
- [2] S. W. Barwick et al., Proc. ICRC 2001, 1101–1104, Hamburg, Germany, (2001).
- [3] W. Wagner et al., Proc. ICRC 2003, 1365–1368, Tsukuba, Japan, (2003).
- [4] T. Messarius et al., These Proceedings, (2005).
- [5] J. Ahrens et al., Nucl. Instrum. Meth., A524:169–194, (2004).